# Relative $g$-factor measurements in $^{54}$Fe, $^{56}$Fe, and $^{58}$Fe

M. C. East,[1] A. E. Stuchbery,[1] S. K. Chamoli,[1] J. S. Pinter,[2] H. L. Crawford,[2] A. N. Wilson,[1,3] T. Kibédi,[1] and P. F. Mantica[2]
[1]*Department of Nuclear Physics, Research School of Physics and Engineering, The Australian National University, Canberra ACT 0200, Australia*
[2]*NSCL and Department of Chemistry, Michigan State University, Michigan 48824, USA*
[3]*Department of Physics, The Australian National University, Canberra, ACT 0200, Australia*
(Received 22 September 2008; published 5 February 2009; publisher error corrected 14 July 2009)

The $g$ factors of the $2_1^+$ states in $^{54}$Fe and $^{58}$Fe have been measured relative to the $2_1^+$ state $g$ factor of $^{56}$Fe using the transient-field technique in inverse kinematics. The results are in satisfactory agreement with recent shell model calculations in the $fp$ model space. For $^{56}$Fe and $^{58}$Fe the $g$ factors approach $Z/A$ and are therefore also consistent with collective interpretations of these $2^+$ states.

DOI: 10.1103/PhysRevC.79.024304 PACS number(s): 21.10.Ky, 27.40.+z, 25.70.De, 23.20.En

## I. INTRODUCTION

Recent advances in computational power for large-basis shell model calculations along with improved shell-model interactions have renewed interest in the $fp$ shell (see, for example, [1,2] and references therein). There has also been renewed effort in testing these calculations through the measurement of $g$ factors of the first $2^+$ states in the even-even nuclei, taking advantage of the improved experimental precision that can be achieved by the use of the transient-field technique in inverse kinematics [3,4].

Whereas the $g$ factors of the $2_1^+$ states of most of the stable even-even isotopes in the $fp$ shell have been measured with considerably improved precision, one exception is $^{58}$Fe. Although stable, $^{58}$Fe has an abundance of only 0.28%, and is not readily produced as a sufficiently intense beam from a natural iron sample by the ion sources in typical tandem laboratories. The previously reported $g$ factors, measured by the transient field in conventional kinematics [5], and by integral perturbed angular correlations in radioactivity [6], have uncertainties of the order of 30%.

We report here a new measurement of $g(2_1^+)$ in $^{58}$Fe, relative to $g(2_1^+)$ in $^{56}$Fe. The case of $^{54}$Fe was also remeasured to compare the present work with recent measurements by the Bonn group [7]. Absolute $g$ factors in these Fe isotopes are obtained by normalization to a new, independent measurement of $g(2_1^+)$ in $^{56}$Fe reported in an accompanying paper [8].

The present experiments are also motivated by measurements [9] at the National Superconducting Cyclotron Laboratory, Michigan State University, which aim to measure the $g$ factors of neutron-rich Fe isotopes toward $^{66}_{26}$Fe$_{40}$ by the high-velocity transient-field technique [10,11]. $^{58}$Fe, which is produced as a strong secondary beam fragment, is the best case to calibrate the transient field at high velocity and thus link the $g$-factor measurements on the stable and neutron-rich Fe isotopes. Our interest in both the stable and neutron-rich isotopes includes the shell structure underlying the development of collective excitations.

## II. EXPERIMENTAL DETAILS

The $g$ factors of the $2_1^+$ states in $^{54,56,58}$Fe were measured by the transient-field technique using projectile excitation and inverse kinematics [3,4]. Beams of $^{54}$Fe, $^{56}$Fe, and $^{58}$Fe at 110 MeV were provided by the Australian National University 14UD Pelletron accelerator. The ion-source samples for the $^{54}$Fe and $^{56}$Fe beams were natural iron powder pressed into standard copper cathodes. Several different samples were used in the course of the measurements: in many cases it was found that the intensity of FeO$^-$ beams exceeded that of Fe$^-$. For the measurements on $^{58}$Fe, separated isotope was mixed with natural iron powder to achieve an enrichment of ∼15% and then pressed into a standard cathode. The relatively low beam energy of ∼2 MeV/nucleon was chosen to ensure that multiple Coulomb excitation of the Fe beams was negligible.

The target described in [8] was used for all three beams. It consisted of a layer of carbon ∼0.6 mg/cm$^2$ thick on a 3.4 mg/cm$^2$ gadolinium foil with an intervening 0.03 mg/cm$^2$ flashing of copper to assist adhesion. A 6.0 mg/cm$^2$ layer of copper on the back of the gadolinium stopped the scattered Fe ions. Additional tantalum foil (4.5 $\mu$m) was placed behind the target to stop the beam. The target was cooled to ∼5 K throughout the experiment as described in more detail in Refs. [8,12]. Beam intensities were kept to about 0.5 pnA. An external magnetic field of 0.09 T magnetized the Gd layer of the target. This field was periodically reversed in direction to minimize systematic errors in the measurement of the precession angles.

The deexciting $\gamma$ rays from the Fe isotopes were measured in coincidence with forward-scattered carbon ions, detected by an array of three silicon photodiode detectors downstream from the target, as described in [8]. One particle detector was centered on the beam axis with the other two placed symmetrically above and below it.

To measure the transient-field precessions, two 50% HPGe detectors and two 12.7 cm by 12.7 cm NaI detectors were placed in pairs at ±65° and ±115° to the beam axis, respectively. The target-detector distances were set such that the detector crystals all subtended a half angle of 18°. The NaI detectors were more than twice as efficient as the Ge detectors for the relevant $\gamma$-ray lines of the even-mass stable Fe isotopes; however the solid angle attenuation coefficients, $Q_k$, were closely matched. Precession data for $^{54}$Fe, $^{56}$Fe, and $^{58}$Fe were taken for ∼1.5 days of beam time per isotope.

Particle-$\gamma$ angular correlations were measured for $^{56}$Fe as reported in [8]. Angular correlations were not measured

 

for $^{54}$Fe and $^{58}$Fe. The mechanism of Coulomb excitation ensures that the angular correlations for $^{54,56,58}$Fe are identical, well within the precision of the measurement. It has been demonstrated that the angular correlations in cases like the present work can be calculated at least as reliably as they can be measured [13–17]. The calculated angular correlations, which are effectively identical for all three isotopes, were therefore used in the following analysis.

## III. RESULTS AND ANALYSIS

### A. Spectra and transient-field precessions

Relative $g$ factors were obtained using analysis procedures similar to those described elsewhere [3,4]. For each direction of the magnetic field, $\gamma$-ray spectra in coincidence with carbon ions were produced. After random subtraction there were no observable contaminants. No excitation to states above the $2_1^+$ state was observed in any of the nuclei studied. Figure 1 shows examples of random-subtracted coincidence $\gamma$-ray spectra.

Figure 2 shows a fit to the Doppler broadened line shape of the 1408 keV transition in $^{54}$Fe from which the lifetime of the $2^+$ state was determined using the code of Wells and Johnson [18]. The result, which combines data for both Ge detectors, is $\tau = 1.04(3)$ ps. The assigned error is statistical only. Our result agrees with $\tau = 1.09(3)$ ps reported by Speidel *et al.* [7] for similar experimental conditions and the same stopping powers [19].

The $g$ factor is proportional to the experimental precession angle, which is given by $\Delta\theta = \epsilon/S$, where $S$ is the logarithmic derivative of the angular correlation at the $\gamma$-ray detection angle. The 'effect,' $\epsilon$, was evaluated [3,4,13] from double ratios of counts in the peaks corresponding to the $2^+ \rightarrow 0^+$ transitions, recorded for field 'up' and field 'down' in the pairs of $\gamma$-ray detectors at $\pm 65^\circ$ and $\pm 115^\circ$.

Data were analyzed for the three particle detectors separately. Due to the symmetry, the experimental observables are the same for the upper and lower (outer) particle detectors. The data for these two detectors can therefore be combined. However both the reaction kinematics and angular correlations differ for the central detector compared with the two outer detectors.

Table I outlines the reaction kinematics and $2_1^+$-state mean lives for the Fe isotopes of interest. Kinematic quantities in this table were evaluated for the experimental conditions by averaging over the energy loss of the beam in the target, and over the solid angles of the particle detectors, with appropriate weighting by the Coulomb-excitation cross sections. Stopping powers are from [19].

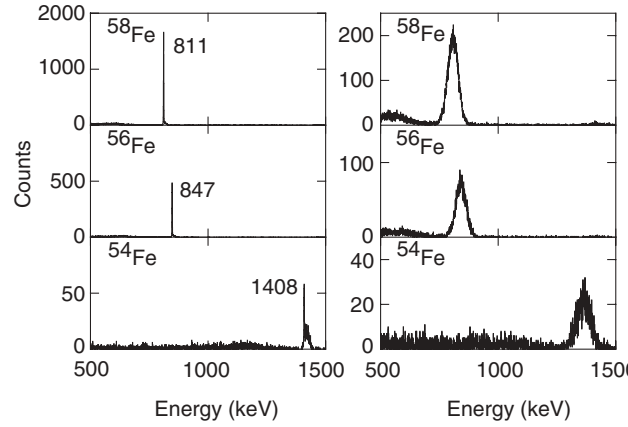


FIG. 1. Spectra observed by $\gamma$-ray detectors at $+65^\circ$ (Ge detector: left panels) and $+115^\circ$ (NaI detector: right panels) in coincidence with the central particle detector. These spectra show the data for magnetic field 'up' collected over a period of ~8 h for $^{56}$Fe and ~32 h for $^{54}$Fe and $^{58}$Fe. The Doppler broadened line shape of the 1408 keV transition is clearly seen in the lower left panel.

The 'correction factor' in the final column of Table I, which is discussed in more detail in the following subsection, is the factor by which the observed precession angles must be multiplied to take into account that the different isotopes traverse the ferromagnetic Gd foil with somewhat different velocities. It also takes into account that some nuclei decay in transit through the ferromagnetic layer before experiencing the full duration of the transient field. This effect is most significant for the case of $^{54}$Fe.

Table II shows a summary of the precession results and relative $g$ factors. To keep this table concise, we have combined the data for the two pairs of $\gamma$-ray detectors, taking advantage of the fact that the 'slopes' $S$ for the NaI and Ge $\gamma$-ray detectors are virtually identical. The relevant (calculated) slopes are: $S_{\text{Center}} = -2.65$ rad$^{-1}$ and $S_{\text{Outer}} = -2.71$ rad$^{-1}$, where the subscripts indicate the particle detector. Because we are concerned with relative measurements, the uncertainties

TABLE I. Reaction kinematics and nuclear properties. $\tau(2_1^+)$ is the mean life of the $2_1^+$ state. $\langle E_i\rangle$ and $\langle E_e\rangle$ are the energies at which Fe ions enter and leave the ferromagnet; $\langle v_i/v_0\rangle$ and $\langle v_e/v_0\rangle$ are the corresponding velocities (Bohr velocity $v_0 = c/137$). $\langle v/v_0\rangle$ is the average velocity for the Fe nucleus in the ferromagnet and $t_{\text{Gd}}$ is the effective time spend in the ferromagnet. The correction factor is $\phi(\infty)_{56}/\phi(\tau)_A$ as described in the text.

| Isotope | $\tau(2_1^+)$[a] (ps) | Particle detector | $\langle E_i\rangle$ (MeV) | $\langle E_e\rangle$ (MeV) | $\langle v_i/v_0\rangle$ | $\langle v_e/v_0\rangle$ | $\langle v/v_0\rangle$ | $t_{\text{Gd}}$ (fs) | Correction factor |
|---|---|---|---|---|---|---|---|---|---|
| $^{54}$Fe | 1.09(3) | Center | 29.2 | 4.1 | 4.66 | 1.75 | 3.03 | 457 | 1.46 |
| | | Outer | 35.7 | 6.4 | 5.16 | 2.18 | 3.55 | 413 | 1.39 |
| $^{56}$Fe | 9.6(4) | Center | 30.7 | 4.9 | 4.70 | 1.87 | 3.05 | 623 | 1.04 |
| | | Outer | 36.9 | 7.2 | 5.16 | 2.27 | 3.52 | 550 | 1.03 |
| $^{58}$Fe | 9.7(3) | Center | 32.0 | 5.6 | 4.71 | 1.97 | 3.13 | 607 | 1.04 |
| | | Outer | 38.1 | 8.0 | 5.14 | 2.36 | 3.57 | 541 | 1.03 |

[a]Mean lives from [7,20].

TABLE II. Summary of precession angles for the $2_1^+$ states of even Fe isotopes. $\langle\Delta\theta\rangle_{\rm Outer}$ is the average precession observed for $\gamma$-rays in coincidence with the outer particle detectors; $\langle\Delta\theta\rangle_{\rm Center}$ is the average precession observed for $\gamma$-rays in coincidence with the center particle detector. The superscript Obs indicates the observed precession values prior to corrections for kinematic conditions and finite level lifetimes. $\langle\Delta\theta\rangle$ is the average precession for all combinations of particle and $\gamma$-ray detectors, corrected for differences in kinematic conditions so that relative precessions are equivalent to relative $g$ factors.

| Isotope | $E(2_1^+)$ (keV) | $\langle\Delta\theta\rangle^{\rm Obs}_{\rm Center}$ (mrad) | $\langle\Delta\theta\rangle^{\rm Obs}_{\rm Outer}$ (mrad) | $\langle\Delta\theta\rangle_{\rm Center}$ (mrad) | $\langle\Delta\theta\rangle_{\rm Outer}$ (mrad) | $\langle\Delta\theta\rangle$ (mrad) | $g(2_1^+)/g(^{56}{\rm Fe})$ |
|---|---|---|---|---|---|---|---|
| $^{54}$Fe | 1408 | −25.4(36) | −25.3(32) | −37.0(53) | −35.1(44) | −35.9(34) | 1.67(17) |
| $^{56}$Fe | 847 | −20.2(12) | −21.4(11) | −21.0(13) | −22.0(12) | −21.6(9) | 1 |
| $^{58}$Fe | 810 | −18.4(13) | −19.7(11) | −19.2(13) | −20.3(14) | −19.8(9) | 0.920(55) |

in the relative slopes (from isotope to isotope) are negligible compared with the statistical uncertainties in the measured precessions.

### B. Velocity-dependence of the transient field

The precession per unit $g$ factor, $\Delta\theta/g \equiv \phi$, is given by

$$\phi(\tau) = -\frac{\mu_N}{\hbar}\int_{t_i}^{t_e} B(v[t])\, e^{-t/\tau}\, dt,$$
$$= -\frac{\mu_N}{\hbar}\int_{E_i}^{E_e} B(v[E])\, e^{-t/\tau}\sqrt{\frac{M}{2E}}\frac{dE}{dE/dx}, \qquad (1)$$

where $B(v)$ is the transient field strength as a function of ion velocity $v$, $E$ is the ion energy, $\tau$ is the mean life of the $2_1^+$ state, $t_{i(e)}$ is the time the Fe ions enter (exit) the Gd layer and $E_{i(e)}$ are the Fe ion energies upon entry into and exit from the Gd layer.

A knowledge of the dependence of the transient-field strength on the ion velocity is needed to correct for the difference in kinematic conditions and the effects of decay in flight through the ferromagnetic layer of the target. It is usual to parametrize the transient field strength in terms of the ion velocity $v$ and atomic number $Z$, assuming that

$$B(v, Z) = aZ^{p_Z}(v/v_0)^{p_v}, \qquad (2)$$

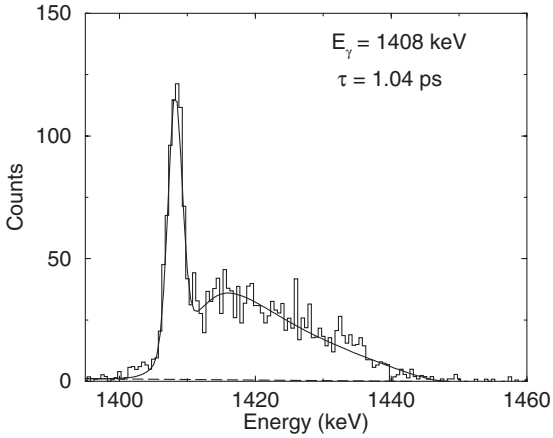


FIG. 2. Fit to the Doppler broadened line shape of the 1408 keV transition in $^{54}$Fe as observed in the detector at +65° to the beam, in coincidence with C ions recorded in the central particle detector. Data for field 'up' and 'down' have been added. The extracted lifetime for the $2^+$ level agrees with that reported by Speidel *et al.* [7].

where $a$, $p_Z$, and $p_v$ are determined from fits to data. Because we are dealing with a single atomic number ($Z = 26$), we are concerned here only with the velocity dependence parameter, $p_v$, for Fe ions. The two most commonly used parametrizations of the transient field differ significantly in this parameter: The 'linear' parametrization [21,22] has $p_v = 1$ whereas the Rutgers parametrization [23] has $p_v = 0.45$.

To our knowledge there have been no studies of the dependence of the transient field on ion velocity under the conditions of the inverse-kinematics reactions used to measure $g$ factors in the $fp$ shell. It is noteworthy therefore that the ratio of precessions for the central and outer particle detectors in the present experiment gives information about the velocity dependence of the transient field. These data are summarized in Table III. The agreement with experiment for $p_v = 1$ is within one standard deviation, whereas experiment is two standard deviations from the parametrization with $p_v = 0.45$.

The correction factor, which appears in the final column of Table I, is defined as $\phi(\infty)_{56}/\phi(\tau)_A$, where the subscript identifies the isotope. The reference, $\phi(\infty)_{56}$, is defined for the case of $^{56}$Fe measured with the central particle detector, and in the limit that there are no decays in flight through the gadolinium foil ($\tau \to \infty$). The correction factor was evaluated assuming that $p_v = 1$; adopting $p_v = 0.45$ would change the resulting $g$-factor ratios by less than 2%.

### C. Relative and absolute $g$ factors

The relative $g$ factors of the $2^+$ states in $^{54}$Fe, $^{56}$Fe, and $^{58}$Fe, as determined in the present and previous [5,7,24] transient-field studies, are summarized in Table IV. Brennan *et al.* [5] measured $g$ factors for all three isotopes using conventional kinematics. Speidel *et al.* have reported a more precise measurement on $^{54}$Fe by exploiting inverse kinematics and calibrating the transient field based on their linear parametrization [7]. The same group also reported precession measurements for $^{56}$Fe under similar kinematic conditions

TABLE III. Ratios of precession angles $\langle\Delta\theta\rangle^{\rm Obs}_{\rm Center}/\langle\Delta\theta\rangle^{\rm Obs}_{\rm Outer}$.

| Isotope | $p_v = 0.45$ | $p_v = 1$ | Experiment |
|---|---|---|---|
| $^{56}$Fe | 1.062 | 0.984 | 0.944(74) |
| $^{58}$Fe | 1.057 | 0.986 | 0.934(84) |
| average: | 1.060 | 0.985 | 0.940(56) |

TABLE IV. Measured $g$-factor ratios for the $2_1^+$ states of even Fe isotopes.

| Ratio | Ref. [5] | Ref. [7] | Present | Average |
|---|---|---|---|---|
| $^{54}$Fe/$^{56}$Fe | 2.7(7) | 1.90(8)[a] | 1.67(17) | 1.87(7) |
| $^{58}$Fe/$^{56}$Fe | 0.75(24) | | 0.920(55) | 0.912(54) |

[a]This value is derived from data in Table I of [24] and results in [7]; see text.

with the same target [24]. The ratio of precessions in [7,24] implies that $g(^{54}\text{Fe})/g(^{56}\text{Fe}) = 1.90(8)$. This ratio takes into account the corrections for decay-in-flight by taking the ratio of the $g$ factor for $^{54}$Fe given in Table I of [7] to the $g$ factor derived for $^{56}$Fe, based on the same transient-field parametrization and results in Table I of [24]. Note that the last two entries of the last column of Table I in [24] report $\Phi^{\text{lin}}$ for $^{56}$Fe, assuming $g = 0.61(8)$, not $\Phi^{\text{lin}}/g$ [25]. (There is a difference in terminology: $\Phi$ in [24] is the same as $\Delta\theta$ here.)

The final column of Table IV combines the present and previous data into adopted values for the relative $g$ factors. To obtain the absolute $g$ factors, we combine the adopted relative $g$ factors with the absolute $g$ factor reported for $^{56}$Fe in the accompanying paper [8], namely $g = +0.509(53)$. Absolute $g$ factors are presented in Table V.

For $^{58}$Fe, aside from the transient-field measurement of Brennan *et al.* [5], there has also been a radioactivity measurement by the integral perturbed angular correlation (IPAC) technique [6]. When the result of that work [6] is corrected to account for more recent lifetime data [20] it becomes $g(2_1^+) = 0.514(118)$. This value is in agreement with the present result. In the final column of Table V we list our adopted $g$ factors for the first excited states in $^{54}$Fe, $^{56}$Fe, and $^{58}$Fe.

## IV. DISCUSSION

There has long been an interest in the collectivity of excited states in the Fe isotopes and the shell structure from which it stems [26]. One of the important themes in recent studies concerns the development of collectivity and the role of the $\nu g_{9/2}$ neutron, which may intrude into the $fp$ shell [1,2,27–33]. For example, the shell gap at $N = 40$ is evidently quenched in neutron-rich nuclei toward $^{66}$Fe$_{40}$ [27,28]. Closer to stability, the role of the $g_{9/2}$ neutron is less pronounced, but may still be present. Deacon *et al.*, who studied the yrast structures in $^{59,60}$Fe, were able to account for the low-lying natural-parity states in both nuclei using the GXPF1 interaction in the full $fp$ model space [32]. However a positive parity band in this nucleus is apparently built on the $g_{9/2}$ orbit, and a negative parity band observed to high spin may be due to the excitation of a pair of $g_{9/2}$ neutrons [32]. In $^{61}$Fe, Hoteling *et al.* [33] had to significantly lower the $\nu g_{9/2}$ single-particle energy (compared with a $^{48}$Ca core), to reproduce the levels above the $9/2^+$ isomeric state in a truncated $fpg$ shell model calculation. There are therefore tantalizing hints concerning the effect of the $g_{9/2}$ neutron on the structure of the Fe isotopes near $^{60}$Fe.

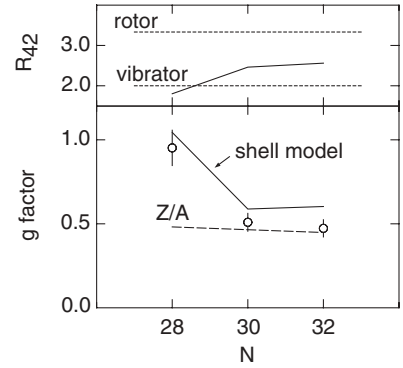


FIG. 3. Upper panel: $R_{42}$ ratios for the isotopes $^{54,56,58}$Fe. Lower panel: Comparison of experimental $2_1^+$ level $g$ factors with $fp$ shell model calculations [1]. The dashed line indicates the collective model estimate, $g = Z/A$.

Figure 3 compares the present adopted $g$ factors with shell model calculations utilizing the GXPF1 interaction in the $fp$ shell [1]. (For the excited states considered here there is little difference between the calculations with bare and effective nucleon $g$ factors in the $M1$ operator.) The upper panel of this figure shows $R_{42} = E(4_1^+)/E(2_1^+)$ as a measure of the evolution of collectivity beyond $N = 28$. For $^{56}$Fe and $^{58}$Fe $R_{42}$ lies between the vibrational and rotational limits.

Agreement between the theoretical and experimental $g$ factors is satisfactory, however the experimental values are all smaller than the theoretical predictions, a difference that appears to increase with $N$. Furthermore, the ratio $g(^{58}\text{Fe})/g(^{56}\text{Fe}) = 0.91(5)$, which is well determined experimentally, does not agree very well with the theoretical ratio of 1.03. For both $^{56}$Fe and $^{58}$Fe, the data are consistent with the collective model estimate of $g = Z/A$. These trends might be an indication of the weakening of the $N = 40$ shell gap

TABLE V. Absolute $g$ factors for the $2_1^+$ states of even Fe isotopes.

| Isotope | $g(A)/g(56)$ | $g(2_1^+)$ | | |
|---|---|---|---|---|
| | | TF[a] | IPAC[b] | Adopted |
| $^{54}$Fe | 1.87(7) | +0.952(105) | | +0.952(105) |
| $^{56}$Fe | 1 | +0.509(53)[c] | | +0.509(53) |
| $^{58}$Fe | 0.912(54) | +0.464(56) | +0.514(118) | +0.473(51) |

[a]Present and previous transient-field studies normalized to the adopted average value for $^{56}$Fe.
[b]Integral perturbed angular correlation measurement from [6].
[c]Normalization value adopted from [8].

and the collective-driving influence of the $\nu g_{9/2}$ orbital, even at $N = 34$.

As discussed previously [7], the $g$ factor for the $N = 28$ nucleus $^{54}$Fe is near unity, indicative of a predominantly proton excitation. The value $g = 0.952(105)$, however, is quenched significantly compared with the Schmidt value for a pure $f_{7/2}$ proton configuration, $g = 1.655$. Thus the $g$ factors show that the wave functions of the $2^+$ states in the Fe isotopes are mixed both at and near $N = 28$.

## V. SUMMARY AND CONCLUSION

The ratio of $g(2_1^+)$ values in $^{58}$Fe and $^{56}$Fe has been measured with considerably improved precision by the transient-field technique. Absolute $g$ factors were obtained by reference to a new independent measurement of the $g$ factor in $^{56}$Fe [8]. The results for $^{56}$Fe and $^{58}$Fe approach the collective estimate of $g = Z/A$ with $g(^{58}\text{Fe}) < g(^{56}\text{Fe})$. They are smaller in magnitude than shell model values calculated for the full $fp$ shell. It is suggested, tentatively, that these trends may point to some weakening of the $N = 40$ shell gap in the Fe isotopes already at $N = 32$. Sensitivity to the strength of the $N = 40$ shell gap will certainly increase for $g$-factor measurements on neutron-rich isotopes approaching $^{66}$Fe.

## ACKNOWLEDGMENTS

The authors are grateful to the academic and technical staff of the Department of Nuclear Physics (Australian National University) for their support. We also thank Andrea Jungclaus for assistance with the LIFETIME code. This work was supported in part by the Australian Research Council Discovery Scheme Grant No. DP0773273 and National Science Foundation Grant No. PHY-06-06007. M.C.E. is supported by an Australian Postgraduate Research Award (APRA).

[1] M. Honma, T. Otsuka, B. A. Brown, and T. Mizusaki, Phys. Rev. C **69**, 034335 (2004).
[2] E. Caurier, G. Martinez-Pinedo, F. Nowacki, A. Poves, and A. P. Zuker, Rev. Mod. Phys. **77**, 427 (2005).
[3] K.-H. Speidel, O. Kenn, and F. Nowacki, Prog. Part. Nucl. Phys. **49**, 91 (2002).
[4] N. Benczer-Koller and G. J. Kumbartzki, J. Phys. G: Nucl. Part. Phys. **34**, R321 (2007).
[5] J. M. Brennan, N. Benczer-Koller, M. Hass, and H. T. King, Phys. Rev. C **16**, 899 (1977).
[6] V. Singh, P. N. Tandon, S. H. Devare, and H. G. Devare, Nucl. Phys. **A137**, 278 (1969).
[7] K.-H. Speidel, R. Ernst, O. Kenn, J. Gerber, P. Maier-Komor, N. Benczer-Koller, G. J. Kumbartzki, L. Zamick, M. S. Fayache, and Y. Y. Sharon, Phys. Rev. C **62**, 031301(R) (2000).
[8] M. C. East, A. E. Stuchbery, S. K. Chamoli, A. N. Wilson, H. L. Crawford, J. S. Pinter, T. Kibédi, and P. F. Mantica, Phys. Rev. C **79**, 024303 (2009).
[9] A. E. Stuchbery *et al.*, NSCL experiment 06013.
[10] A. D. Davies, A. E. Stuchbery, P. F. Mantica, P. M. Davidson, A. N. Wilson, A. Becerril, B. A. Brown, C. M. Campbell, J. M. Cook, D. C. Dinca *et al.*, Phys. Rev. Lett. **96**, 112503 (2006).
[11] A. E. Stuchbery, A. D. Davies, P. F. Mantica, P. M. Davidson, A. N. Wilson, A. Becerril, B. A. Brown, C. M. Campbell, J. M. Cook, D. C. Dinca *et al.*, Phys. Rev. C **74**, 054307 (2006).
[12] A. E. Stuchbery, A. B. Harding, D. C. Weisser, N. R. Lobanov, and M. C. East (in preparation).
[13] A. E. Stuchbery, A. Nakamura, A. N. Wilson, P. M. Davidson, H. Watanabe, and A. I. Levon, Phys. Rev. C **76**, 034306 (2007).
[14] A. E. Stuchbery, I. Morrison, L. D. Wood, R. A. Bark, H. Yamada, and H. H. Bolotin, Nucl. Phys. **A435**, 635 (1985).
[15] A. E. Stuchbery, G. J. Lampard, and H. H. Bolotin, Nucl. Phys. **A528**, 447 (1991).
[16] S. S. Anderssen, A. E. Stuchbery, and S. Kuyucak, Nucl. Phys. **A593**, 212 (1995).
[17] P. F. Mantica, A. E. Stuchbery, D. E. Groh, J. I. Prisciandaro, and M. P. Robinson, Phys. Rev. C **63**, 034312 (2001).
[18] J. C. Wells and N. R. Johnson, program LINESHAPE, ORNL (1994).
[19] J. F. Ziegler, J. P. Biersack, and U. Littmark, in "The Stopping and Range of Ions in Solids," Vol. 1 of *The Stopping and Ranges of Ions in Matter*, edited by J. F. Ziegler (Permagon, New York, 1985).
[20] S. Raman, C. W. Nestor, and P. Tikkanen, At. Data Nucl. Data Tables **78**, 1 (2001).
[21] J. L. Eberhardt, R. E. Horstman, P. C. Zalm, H. A. Doubt, and G. van Middelkoop, Hyperfine Interact. **3**, 195 (1977).
[22] K.-H. Speidel, U. Reuter, J. Cub, W. Karle, F. Passek, H. Busch, S. Kremeyer, and J. Gerber, Z. Phys. D **22**, 371 (1991).
[23] N. K. B. Shu, D. Melnik, J. M. Brennan, W. Semmler, and N. Benczer-Koller, Phys. Rev. C **21**, 1828 (1980).
[24] R. Ernst, K. H. Speidel, O. Kenn, A. Gohla, U. Nachum, J. Gerber, P. Maier-Komor, N. Benczer-Koller, G. J. Kumbartzki, G. Jakob *et al.*, Phys. Rev. C **62**, 024305 (2000).
[25] K.-H. Speidel (private communication, 2008).
[26] J. B. McGrory and S. Raman, Phys. Rev. C **20**, 830 (1979).
[27] M. Hannawald, T. Kautzsch, A. Wöhr, W. B. Walters, K.-L. Kratz, V. N. Fedoseyev, V. I. Mishin, W. Böhmer, B. Pfeiffer, V. Sebastian *et al.*, Phys. Rev. Lett. **82**, 1391 (1999).
[28] E. Caurier, F. Nowacki, and A. Poves, Eur. Phys. J. A **15**, 145 (2002).
[29] I. Matea, G. Georgiev, J. M. Daugas, M. Hass, G. Neyens, R. Astabatyan, L. T. Baby, D. L. Balabanski, G. Bélier, D. Borremans *et al.*, Phys. Rev. Lett. **93**, 142503 (2004).
[30] N. Vermeulen, S. K. Chamoli, J. M. Daugas, M. Hass, D. L. Balabanski, J. P. Delaroche, F. de Oliveira-Santos, G. Georgiev, M. Girod, G. Goldring *et al.*, Phys. Rev. C **75**, 051302(R) (2007).
[31] S. Lunardi, S. M. Lenzi, F. D. Vedova, E. Farnea, A. Gadea, N. Mărginean, D. Bazzacco, S. Beghini, P. G. Bizzeti, A. M. Bizzeti-Sona *et al.*, Phys. Rev. C **76**, 034303 (2007).
[32] A. N. Deacon, S. J. Freeman, R. V. F. Janssens, M. Honma, M. P. Carpenter, P. Chowdhury, T. Lauritsen, C. J. Lister, D. Deweryniak, J. F. Smith *et al.*, Phys. Rev. C **76**, 054303 (2007).
[33] N. Hoteling, W. B. Walters, R. V. F. Janssens, R. Broda, M. P. Carpenter, B. Fornal, A. A. Hecht, M. Hjorth-Jensen, W. Królas, T. Lauritsen *et al.*, Phys. Rev. C **77**, 044314 (2008).